Accuracy of Potential Flow Methods to Solve Real-time Ship-Tug Interaction Effects within Ship Handling Simulators

B. N. Jayarathne, D. Ranmuthugala, S. Chai & J. Fei
Australian Maritime College, University of Tasmania, Newnham, Tasmania, Australia

ABSTRACT: The hydrodynamic interaction effects between two vessels that are significantly different in size operating in close proximity can adversely affect the safety and handling of these vessels. Many ship handling simulator designers implement Potential Flow (PF) solvers to calculate real-time interaction effects. However, these PF solvers struggle to accurately predict the complicated flow regimes that can occur, for example as the flow passes a wet transom hull or one with a drift angle. When it comes to predicting the interaction effects on a tug during a ship assist, it is essential to consider the rapid changes of the tug's drift angle, as the hull acts against the inflow creating a complicated flow regime. This paper investigates the ability of the commercial PF solver, Futureship®, to predict the accurate interaction effects acting on tugs operating at a drift angle during ship handling operations through a case study. This includes a comparison against Computation Fluid Dynamics (CFD) simulations and captive model tests to examine the suitability of the PF method for such duties. Although the PF solver can be tuned to solve streamline bodies, it needs further improvement to deal with hulls at drift angles.

1 INTRODUCTION.

Tug boats play a significant role when ships incapable of slow manoeuvres are handled in restricted waters. Ships and their attending tugs are exposed to dangers such as collision, grounding, girting, and run-overs when operating in close proximity in restricted waterways. Furthermore, the hydrodynamic interaction forces and moments can adversely affect the handling and safety of the attending tugs. Hensen (2012) showed that the interaction effects change with ship type, width of fairway, and the drift angles of the vessels; which can cause even experienced tug masters difficulties in identifying safe operating envelopes for their tugs during such manoeuvres. In addition, Hensen (2012) stated that these effects become prominent when the vessels were significantly dissimilar in size and operated in close proximity during tight manoeuvres. Hensen, Merkelbach, and Wijnen (2013) questioned 160 tug masters with regard to their awareness of the interaction effects during such manoeuvres. Around 30% of the tug masters had faced critical situations due to unexpected ship-to-ship interaction effects in actual ship-assist manoeuvres.

Ship handling simulators use empirical and semi-empirical methods, theoretical and numerical methods, or potential flow methods to predict interaction effects: (Sutulo & Soares, 2009). With the exception of the latter, the others require an interaction effect coefficients database to solve mathematical models fed into the simulators, with the database developed and validated by empirical and numerical techniques. For example Vantorre, Verzhbitskaya, and Laforce (2002) conducted physical

model tests to determine the ship interaction effects in head-on and overtaking encounters of similar and dissimilar ships. The test results were used to create a new mathematical model to improve the quality of the interaction effects within ship manoeuvring simulators.

Researchers such as Sutulo and Soares (2009), Sutulo, Soares, and Otzen (2012) and Pinkster and Bhawsinka (2013) employing Potential Flow (PF) solvers to predict the interaction effects as an alternative to the excessive work and high cost involved in developing a coefficient based model. Currently only the relatively simple PF double-body panel method is utilised to provide estimates of the interaction forces and moments in real time within simulators (Sutulo et al., 2012). Pinkster and Bhawsinka (2013) developed a computer program to estimate and validate the interaction effects using the simulator operated by the Maritime Research Institute Netherland (MARIN). The PF double-body method was employed within their computer program for multi-body cases involving ships and port structures. Real time interaction forces and moments were fed into the simulator using high speed computers to solve the flow equations. However, the final results were found to be highly sensitive to the initial conditions, which were tedious to setup.

Sutulo et al. (2012) developed a PF double-body panel code on the basis of the classic Hess and Smith method to estimate interaction effects in real time on commonly used computer hardware. The results obtained with the code were validated against experimental data obtained in deep and shallow water towing tanks for a tug operating near a larger vessel. The results illustrated the potential of the PF double-body panel method for predicting interaction effects, while highlighting the lack of accuracy in predicting the sway forces at small horizontal clearances, which were expected to be more pronounced in non-parallel operations, similar to those encountered during tugs assisting ships. Fonfach, Sutulo, and Soares (2011) did experimental and numerical investigations to explore the contribution of various factors to interaction effects, which were not accounted for by the PF method. They revealed substantial influence of free-surface effects on the accuracy of predicted interaction effects.

Many researchers (Doctors, 2006; Doctors & Beck, 2005; Eliasson & Olsson, 2011; Mantzaris, 1998; Mierlo, 2006; Pranzitelli, Nicola, & Miranda, 2011) have investigated the capabilities of PF methods to study various hull shapes, especially transom stern hulls with free surface. Pranzitelli et al. (2011) studied the free-surface flow around a semi-displacing transom stern motor-yacht advancing steadily in calm water using both PF method and Computational Fluid Dynamics (CFD), and comparing them to Experimental Fluid Dynamics (EFD) results. It was found that the results generated from the PF method were substantially different because of the inability of its panels to 'roll-down' and intersect with each other during iterations. The researchers concluded that the presence of the free-surface can make more complicated discretisation, resulting in numerical problems for complex geometries, such as for transom stern hulls.

Considering the interaction effects on a tug during ship assist, the rapid changes of tug drift angle causes a large portion of the downstream wake due to the hull to be characterised by a bluff body flow in a similar manner to a wet transom flow, as shown in Figure 1.Thus, it is essential to select a flow solver that can accurately solve such conditions during real-time predictions. Therefore, this study aims to examine the accuracy of the drag force prediction of the commercial PF package Futureship®, in wet transom conditions as a case study to investigate its suitability to use in complicated real-time interaction effects analysis of tugs operating at a drift angle.
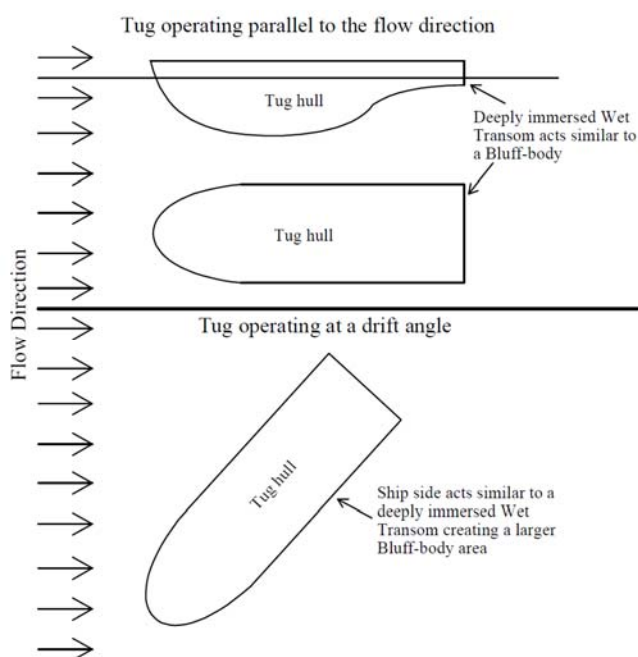

Figure 1. Tug operating parallel to the flow (top) and operating at a drift angle (bottom)

FS-Flow® is the module used within Futureship® for Rankine-Source panel code analysis (DNV GL Maritime, 2014) and it solves the boundary value problem of potential theory including nonlinear free-surface. The potential flow approach assumes that the fluid is inviscid and the flow is irrotational around the bodies. Hence, FS-Flow® is equipped with a separate module capable of calculating the viscous resistance in terms of a friction line in combination with the wavy wetted hull surface. Therefore, the dynamic forces, static forces, and viscous forces acting on the bodies are included in the final results, although the fluid is considered as inviscid within potential flow. The total resistance and its components obtained from the PF solver was then compared against captive model experiments and CFD results generated by the commercial CFD code Star-CCM+® to investigate the possibility of using the PF software for future analysis of interaction effects.

2 NUMERICAL ANALYSIS

The setup and relevant features of the two commercial software packages, FS-Flow® and Star-CCM+®, are provided below.

2.1 Hull Form and Coordinate System

A 1:20 scaled hull model of the Australian Maritime College's (AMC) 35m training vessel *TV Bluefin* was utilised in this study. The particulars of the full and model scale hulls are given in Table 1. The two test conditions analysed to investigate the effects of transom generated complex flow regimes were:
- dry transom with a model draft of 0.17m; and
- wet transom with a model draft of 0.18m.

Table 1. Main Particulars of the Hull Form

Main Particulars	Unit	Full Scale	Model Scale
Length Waterline, L	m	32.150	1.608
Wetted Surface area, S	m²	384.15	0.96
Dry Transom Draft	m	3.48	0.17
Wet Transom Draft	m	3.60	0.18

A three-dimensional model scale hull form was developed using the commercial software Rhinoceros® V5.0 and imported into the two packages. The coordinate system for the analysis is shown in Figure 2. The flow velocity vector was in the positive X direction while the horizontal plane through the origin was considered as the free surface.

2.2 Domain and Mesh in FS-Flow®

Flow velocities ranged from 0.34m/s to 1.04m/s in model scale, acting along the positive X direction, with the vessel allowed to trim and heave during the analysis. The free surface had a rectangular shape, with the inlet boundary at a distance equal to the scaled model waterline length (L_m) upstream of the origin, the outlet boundary at $3L_m$ downstream from the origin, and a total domain width of $1.1L_m$. The dimensions were selected to match those of the AMC towing tank, except for the length, which was shorten to reduce the computational effort without adversely affecting wake resolution. The mesh configuration is illustrated in Figure 2, which was developed in FS-Flow®.
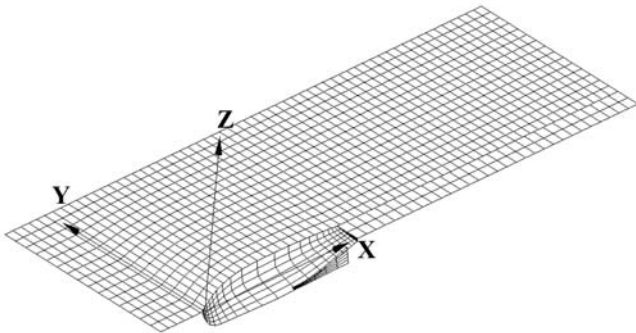

Figure 2. Coordinates and Ship Model with Free surface in FS-Flow®

The mesh independence study was conducted through mesh refinements without affecting the stability of the solver. The drag coefficient at a forward speed of 1.04m/s was tested for dry transom condition for the models with different panel numbers to obtain an appropriate mesh. This approach provided sufficiently accurate results while maintaining low computational effort. The finest mesh investigated had 4220 panels; while a 3490

panel mesh was selected as a suitable mesh for steady-state simulations as its predictions were within 1.5% of that for the finest mesh (see Figure 3).
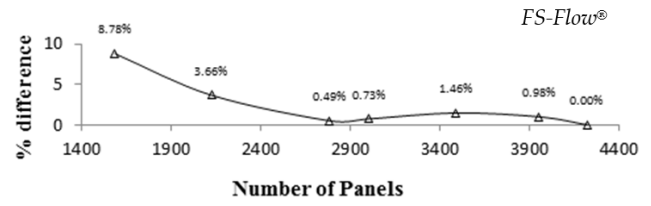

Figure 3. Absolute % difference of Drag Coefficient against finest panel mesh for the FS-Flow® model

2.3 Setup and Mesh in Star-CCM+®

Star-CCM+® uses a finite volume technique to solve the Reynolds Averaged Navier-Stokes (RANS) equations (CD-Adapco, 2014). In order to directly compare the CFD and EFD results, the width and depth of the AMC towing tank were replicated in the numerical fluid domain, although the length was reduced to 10.0m to decrease the mesh load while ensuring the pressure and wake fields generated by the hull were sufficiently resolved within the domain. In addition, since the flow around the hull is symmetrical about the centerline, only the starboard half of the hull was modeled in order to reduce the computational domain and thus the associated computational effort. The vessel was fixed in all degrees of freedom, using particular trim and heave conditions obtained from the FS-Flow® simulation results. The computations were performed using hexahedral trimmed mesh generated by Star-CCM+®. Following a mesh independence study (Figure 4), a mesh with approximately 3.5 million cells was selected for the investigation as the percentage difference reduced to below 0.5% beyond this size mesh.

The near wall spacing on the vessel is defined using the dimensionless distance (y^+) measured from the wall surface to the edge of the first layer. The resolution of the boundary layer was estimated by prescribing the number of inflation prisms layers, the growth rate, and the first node distance from the wall (δy) reflected by the non-dimensional distance value (y^+) as defined in equation (1).

$$\delta y = L_m \times y^+ \times \sqrt{80} R_e^{\left(\frac{-13}{14}\right)} \qquad (1)$$

The minimum total thickness of the inflation layers around the hull was matched to 2 times Prandtl's 1/7th power law of theoretical estimate of turbulent boundary layer thickness over a flat plate, i.e. 2×0.16 $L_m / R_e^{1/7}$ (White, 2003).

The y^+ study was conducted between y^+~1 to y^+~100 with the k-ω SST turbulence model, which change from the low Reynolds wall treatment model to the empirical-based wall function formulation around y^+=10. From Figure 5 it is seen that the % variation of the drag coefficient is around 5% at a y^+ of 30. Thus, y^+~30 was selected as a compromise between accuracy and the solver time and effort. However, it should be noted that this y^+ value is

acceptable for longitudinal flow, but too high for oblique flow which would need a y^+ less than 1 (Leong et al., 2014). Customised anisotropic refinement was applied to the free-surface region (Figure 6) to resolve the wave field around the hull.
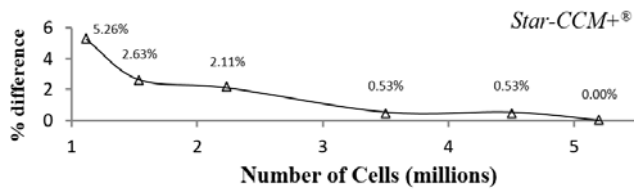

Figure 4. CFD grid independent study: Absolute % difference of Drag Coefficient against finest mesh
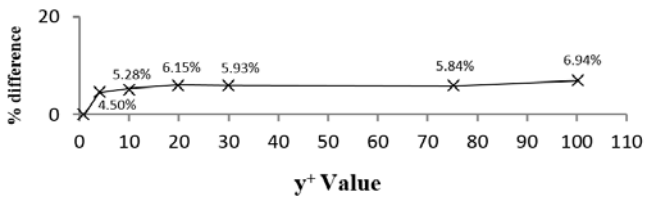

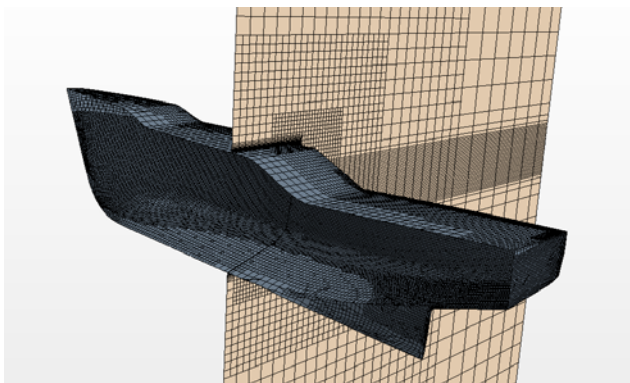Figure 5. CFD near wall mesh (y^+) study: % difference of Drag Coefficient against y^+~1mesh

Figure 6. Hexahedral Mesh used in Star-CCM+®

Simulations were treated as implicit unsteady, conducted for 25s durations with a 0.024s time step and 10 inner iterations. The free surface was modelled as an Euler Multiphase and the volume of fluid technique, with the inflow considered as a flat wave having particular velocity. The drag force acting on the vessel was calculated for similar speeds and drafts as done for FS-Flow®.

3 EXPERIMENTAL SETUP

Captive scaled model experiments were performed in AMC's 100m (length) x 3.55m (width) x 1.5m (depth) towing tank (Figure 7). The scaled hull model, which was allowed to trim and heave, was attached below the towing carriage using one strain gauge and two Linear Voltage Displacement Transducers (LVDTs). Experiments were conducted for the two different drafts of the hull model. At the lower 0.17m draft the transom was in the dry condition, while at the higher 0.18m draft it was wet. Both conditions were tested at speeds ranging from 0.34m/s to 1.04m/s in model scale.
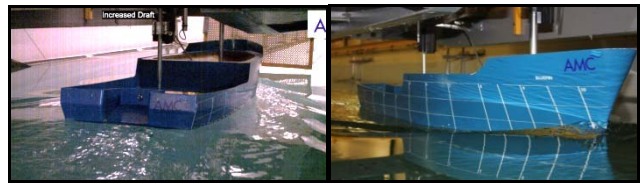

Figure 7. Experimental testing in AMC Towing Tank; left - stern view, right – bow view

4 RESULTS AND DISCUSSION

4.1 *Drag Coefficient and Friction Coefficient*

The drag forces obtained from the numerical and experimental work were non-dimensionalised to obtain the drag coefficient *(C_T)* as shown in Eq. (2). The frictional resistance coefficients *(C_F)* given in Eq. (3) obtained from the numerical results were compared against the ITTC correlation line given in Eq. (4) (ITTC, 2011).

$$C_T = \frac{R_T}{\frac{1}{2}\rho S V^2} \tag{2}$$

$$C_F = \frac{R_F}{\frac{1}{2}\rho S V^2} \tag{3}$$

$$ITTC\ correlation\ line = \left(1 + 0.1194\right)\frac{0.067}{\left(\log_{10} R_e - 2\right)^2} \tag{4}$$

with the definitions given in the Nomenclature at the end of this paper.

4.1.1 *Dry transom with a model draft of 0.17m*

In this condition the transom remained dry above the waterline, giving a streamlined water-plane. The non-dimensionalised drag force results from EFD, PF code FS-Flow® (PF), and CFD are plotted against the Length Froude number *(F_n)* in Figure 8.

The numerical and EFD results have a similar trend except at lower F_n, where the numerical models tend to over-predict. This may be due to the non-accurate prediction of laminar to turbulent transient region on the scaled experimental model. However, the PF and CFD remain similar even at low F_n, with the maximum difference between the PF and CFD results being 15%, while the maximum difference between the PF and EFD results is 7.2%, except at the lowest F_n as discussed above.
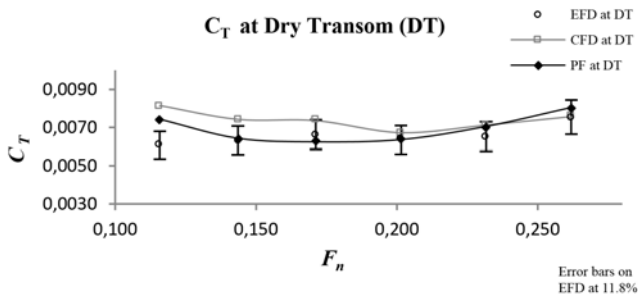
Figure 8. C_T comparison for dry transom condition

The results indicate that the viscous module integrated within FS-Flow® has good prediction capability. In order to verify its accuracy, the frictional coefficients (C_F) obtained from the PF and CFD simulations were compared against the ITTC correlation line as shown in Figure 9. The C_F from the PF method correlates well with the ITTC line with a maximum difference of 5%, whereas the CFD values are slightly below the ITTC prediction with an average difference of 15%. A finer mesh with different turbulence models and a smaller y^+ may improve the CFD results. This was not carried out since the aim of the study was to investigate the accuracy of the PF solver. From the current work it is clear that the PF solver in FS-Flow® is suitable to solve flow around well streamlined hull geometries.
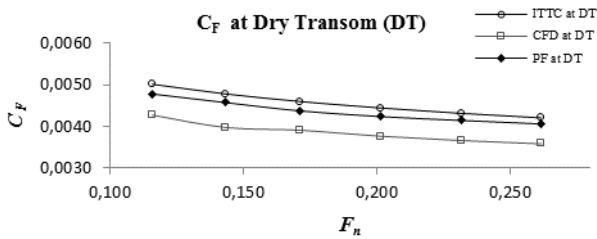

Figure 9. C_F comparison for dry transom condition

4.1.2 Wet transom with a model draft of 0.18m

In order to test FS-Flow®'s ability to solve wet transom conditions, the model was tested at the higher draft. The non dimensionalised EFD, CFD, and PF drag forces in this condition are plotted against F_n in Figure 10.
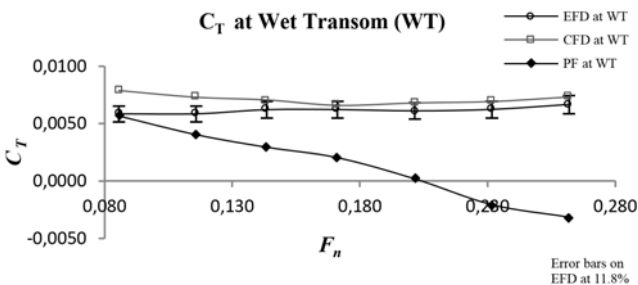

Figure 10. C_T comparison for wet transom condition

It is evident that the CFD and EFD results are in good agreement throughout the F_n range. However, the PF results, although is relatively close to the EFD at low F_n, it significantly under predicts C_T as F_n increases. Interestingly, the direction of C_T changes around F_n of 0.2, causing the drag force on the vessel

to act opposite to the flow direction, a physical impossibility. Since the total drag is made up of viscous, pressure, and wave making components, it is necessary to decompose the resistance in the different components to identify the real cause for this discrepancy.

First considering the viscous drag force, a comparison was made between those obtained by the PF solver, the CFD shear force, and the ITTC correlation line, presented in Figure 11. It is apparent that the viscous force generated by PF is in agreement with the ITTC correlation line, which is similar to the results obtained in the dry transom conditions as discussed in section 4.1.1.
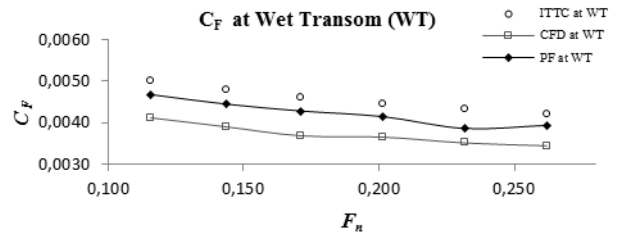

Figure 11. C_F comparison for Wet Transom condition

4.2 Wave Pattern and Pressure Contour

Since the results discrepancy was not related to the viscous effects, the residuary components were next investigated, especially as the error increased significantly with F_n. Thus, the free surface wave patterns generated by the PF and CFD simulations as well as photographs of the wave patterns from the EFD work at a speed of 1.04m/s were compared to identify the influence of wave making resistance. Figure 12 provides the PF and CFD wave patterns for wave heights between ±0.03m, with Figure 7 providing the EFD patterns.
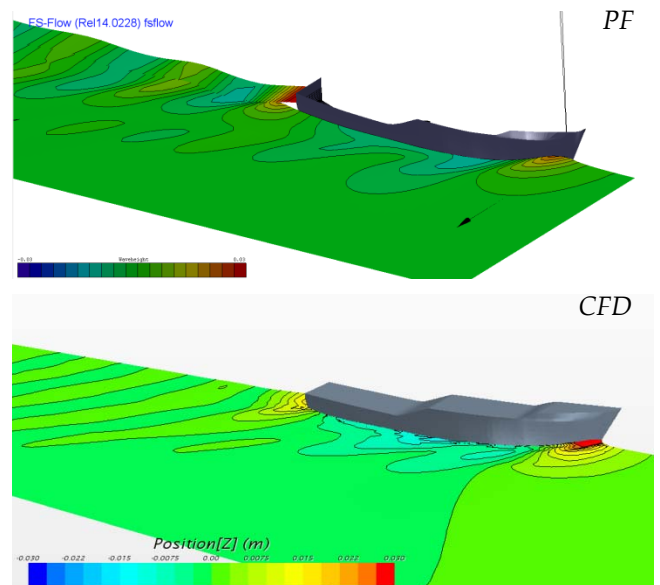

Figure 12. Free surface waves heights in PF & CFD

It is clearly seen from this plots that the waves generated by PF are not in agreement with that obtained from EFD and CFD. Notably, the stern wave generated by PF has the highest magnitude, whereas

the CFD as expected has it for the bow wave, similar to the EFD as seen in the photographs in Figure 7. The inaccurate wave pattern in PF will create a high pressure region at the stern of the hull, which can result in a negative drag force. In order to verify this, the Dynamic Pressure Coefficient (C_P) generated by PF was examined as shown in the Figure 13 (a).
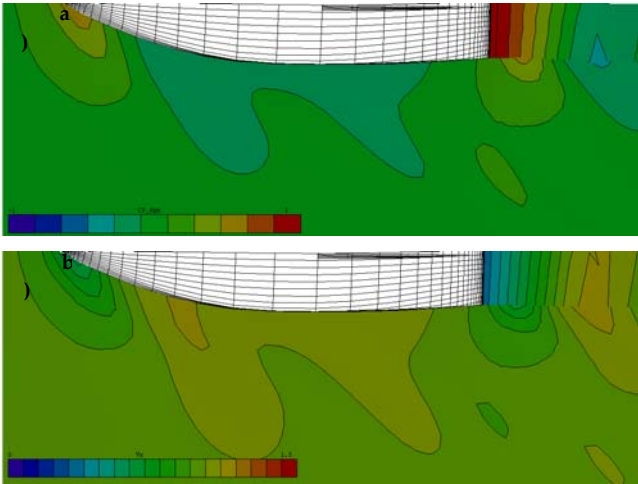

Figure 13: a) Dynamic Pressure Coefficient and b) velocity contour generated by PF

As suspected, the PF code has a high positive pressure region at the stern due to the weakness in predicting the horizontal velocity component within the transom mesh. This creates a very low horizontal velocity at the transom Figure 13 (b), and hence a corresponding high pressure creating the negative drag force on the vessel. Since this unrealistic result occurred due to the wet transom, it was decided to check the drag force generated by the PF code without the transom mesh (Figure 14) at a 0.18m draft, with the results plotted against the F_n in Figure 15.
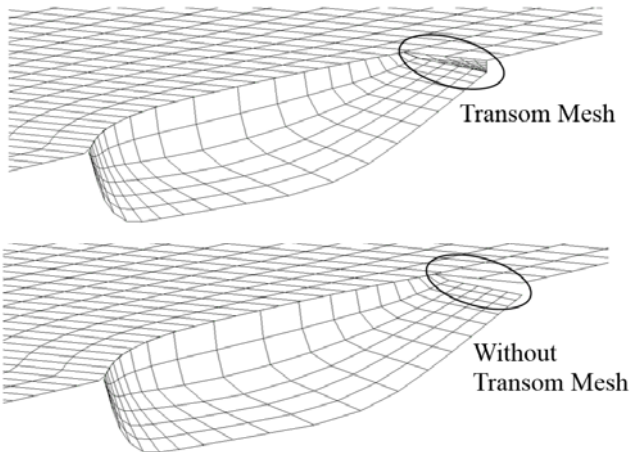

Figure 14. PF hull with (top) and without (bottom) transom mesh

4.3   Results without Transom Mesh

It is interesting to note that when the transom mesh is omitted from the hull, the accuracy of the drag force predicted by the PF simulation is appreciably improved showing good agreement with the EFD and CFD results. Removing the transom mesh mitigated

the error attributed to insufficient resolution of the large pressure gradient on the hull and poor numerical conditioning of the pressure integration.
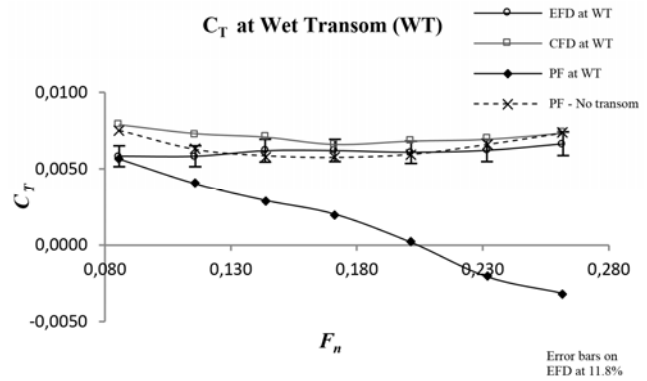

Figure 15. Comparison for wet transom condition, including the PF mesh without the transom mesh

Thus, it is noted that the PF code is unable to solve flow equations on transverse panels which block the flow streamlines creating breaking and spraying waves. However, reasonable results can be obtained for wet transom geometries if the transom mesh is omitted.

Thus, it is important to investigate the possibility of utilising this finding to conduct interaction effects analysis during ship handling operations. During such operations, tugs can dramatically change their drift angle to maintain the course of the ship. If the PF code is used to solve such cases, the panel generation has to be done as shown in Figure 16.
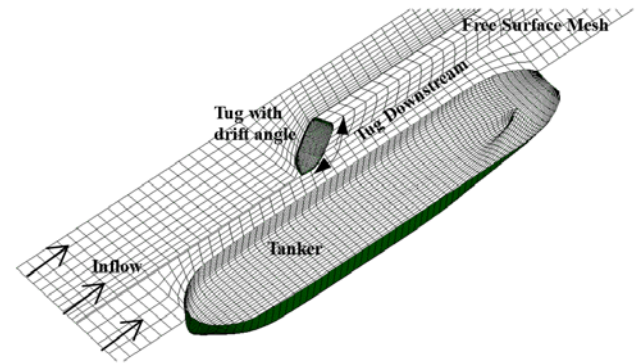

Figure 16. Ship Handling Operation: Panel generation in PF

As illustrated in Figure 16, when the tug drift angle changes, a large portion of the downstream wake due to the tug hull is characterised by a stagnation pressure created due to a bluff body similar to a wet transom. This downstream area is due to a large portion of the vessel's downstream side hull. Thus, if the technique of omitting the downstream transverse mesh panels to improve results is utilised, a significant part of the hull mesh would be omitted, unlike in the inline flow condition where the transom is a relatively small mesh panel. This would result in accuracy and stability issues within the PF simulation. Thus, the dynamic pressure prediction algorithm in FS-Flow® is not capable of handling non-streamlined geometries and it needs further improvements to solve complicated interaction effects.

5 CONCLUSION

In this paper the drag forces acting on a transom stern hull operating under wet and dry transom conditions were investigated using PF, CFD, and EFD methods. The aim was to identify the accuracy of the PF method to determine real-time interaction effects acting on a tug operating in close proximity to a tanker within ship handling simulators. For the dry transom flow, the PF solver showed very good agreement with the EFD and CFD results. However, it failed to do so for the wet transom condition, especially at higher F_n. Further investigations revealed that these discrepancies were due to its weaknesses in predicting the flow velocity around the transom panel mesh, which was at near right angles to the flow direction.

It was identified that if FS-Flow® is used to solve drag forces on wet transom hulls of tugs operating parallel to the flow, it is necessary to omit the transom stern mesh panel. Thus it is suitable to estimate the forces acting on well streamlined bodies across the length based F_n range, including the viscous effects. However, this is not feasible when the tug is at a drift angle, as the mesh panel affected will represent one full side of the vessel, thus adversely affecting the mesh domain. Therefore, it was identified that the investigated PF solver, FS-Flow®, is limited in its ability to predict real-time interaction effects within ship handling simulators, especially in manoeuvrers such as tug assist operations.

Currently the authors are conducting CFD studies to predict the offline interaction effects acting on a tug with varying drift angles operating in close proximity to a large tanker, with validation through EFD. The quantified results will be fed into AMC's ship handling simulator via a database in order to predict real-time interaction effects.

NOMENCLATURE

AMC — Australian Maritime College

CFD — Computational Fluid Dynamics

C_F — friction coefficient *(dimensionless)*

C_P — dynamic pressure coefficient *(dimensionless)*,

$$C_p = \left(P - P_\infty\right)/q$$

C_T — drag coefficient *(dimensionless)*

DT — dry transom

EFD — Experimental Fluid Dynamics

F_n — Length Froude Number *(dimensionless)*,

$$F_n = V / \sqrt{gL_m}$$

g — gravity *(9.81m/s²)*

ITTC — International Towing Tank Conference

L_m — length of the ship model *(m)*

P — pressure *(pa)*

PF — Potential Flow code FS-Flow

P_∞ — free-stream reference pressure *(pa)*

q — dynamic pressure, $q = \rho V^2 / 2$ *(pa)*

R_e — Reynolds Number *(dimensionless)*,

$$R_e = VL_m / v$$

R_F — frictional resistance on ship model *(N)*

R_T — total resistance on ship model *(N)*

S — wetted surface area of ship model *(m²)*

V — velocity of ship model *(0.34m/s to 1.04m/s)*

WT — wet transom

y^+ — near wall mesh spacing *(dimensionless)*

δy — first node wall distance of the near wall mesh *(m)*

v — kinematic viscosity of water *(1.00x10⁶ m²/s)*

ρ — density of water *(1000 kg/m³)*

REFERENCES

CD-Adapco. (2014). User Manual of Star CCM+ Version 08.

DNV GL Maritime. (2014). User Manual of FS-Flow Version 14.0228.

Doctors, L. J. (2006). *A Numerical Study of the Resistance of Transom Stern Monohulls.* Paper presented at the 5th International Conference on High Performance Marine Vehicles, Australia.

Doctors, L. J., & Beck, R. F. (2005). *The Separation of the Flow Past a Transom Stern.* Paper presented at the First International Conference on Marine Research and Transportation (ICMRT '05), Ischia, Italy.

Eliasson, S., & Olsson, D. (2011). *Barge Stern Optimization: Analysis on a Straight Shaped Stern using CFD.* (MSc thesis), Chalmers University of Technology, Gothenburg, Sweden. (X-11/266)

Fonfach, J. M. A., Sutulo, S., & Soares, C. G. (2011). *Numerical study of Ship to Ship Interaction Forces on the Basis of Various Flow Models.* Paper presented at the 2nd International Conference on Ship Manoeuvring in Shallow and Confined Water: Ship to Ship Interaction, Trondheim, Norway.

Hensen, H. (2012). Safe Tug Operation: Who Takes the Lead? *International Tug & OSV, 2012*(July/August), 70-76.

Hensen, H., Merkelbach, D., & Wijnen, F. V. (2013). Report on Safe Tug Procedures (pp. 40). Netherlands: Dutch Safety Board.

ITTC. (2011). Resistance Test (Vol. 7.5-02-02-01): International Towing Tank Conference.

Leong, Z. Q., Ranmuthugala, D., Penesis, I., & Nguyen, H. (2014). RANS-Based CFD Prediction of the Hydrodynamic Coefficients of DARPA SUBOFF Geometry in Straight-Line and Rotating Arm Manoeuvres. *Transactions RINA: Part A1- International Journal Maritime Engineering*.

Mantzaris, D. A. (1998). *A Rankine Panel Method as a Tool for the Hydrodynamic Design of Complex Marine Vehicles.*

(Ph.D. thesis), Massachusetts Institute of Technology, USA.

Mierlo, K. V. (2006). *Trend Validation of SHIPFLOW based on the Bare Hull Upright Resistance of the Delft Series.* (MSc thesis), Delft University of Technology, Netherlands.

Pinkster, J. A., & Bhawsinka, K. (2013). *A Real-time Simulation Technique for Ship-Ship and Ship-Port Interactions.* Paper presented at the 28th International Workshop on Water Waves and Floating Bodies (IWWWFB 2013), L'Isle sur la Sorgue, France.

Pranzitelli, A., Nicola, C., & Miranda, S. (2011). *Steady-state calculations of Free Surface Flow around Ship Hulls and Resistance Predictions*. Paper presented at the High Speed Marine Vehicles (IX HSMV), Naples, Italy.

Sutulo, S., & Soares, C. G. (2009). *Simulation of Close-Proximity Maneuvers using an Online 3D Potential Flow Method.* Paper presented at the International Conference on Marine Simulation and Ship Maneuverability, Panama City, Panama.

Sutulo, S., Soares, C. G., & Otzen, J. F. (2012). Validation of Potential-Flow Estimation of Interaction Forces Acting upon Ship Hulls in Parallel Motion. *Journal of Ship Research, 56*(3), 129–145.

Vantorre, M., Verzhbitskaya, E., & Laforce, E. (2002). Model Test Based Formulations of Ship-Ship Interaction Forces. *Ship Technology Research, 49*, 124-141.

White, F. M. (2003). *Fluid Mechanics* (5 ed.). New York: McGraw-Hill.